

Electronic Structure of Zeolites Studied by X-Ray Photoelectron Spectroscopy

YASUAKI OKAMOTO, MANABU OGAWA, AKINORI MAEZAWA,
AND TOSHINOBU IMANAKA

*Department of Chemical Engineering, Faculty of Engineering Science, Osaka University,
Toyonaka, Osaka 560, Japan*

Received August 13, 1987; revised March 14, 1988

The electronic structure of zeolites was systematically investigated by utilizing XPS. Zeolites A, X, Y, and mordenites in their sodium and decationized forms as well as the series of alkali metal cation-exchanged X and Y zeolites were examined. The electronic structure of zeolites was demonstrated to depend strongly on both the composition and the cation involved. It is suggested that the basic strength of framework oxygen increases with increasing Al content regardless of the crystal structure and with the decreasing electronegativity of the counter cation. These results explain well certain catalytic properties of alkali metal cation-exchanged zeolites. On the basis of the XPS results, the nature of chemical bonding in zeolites is discussed. © 1988 Academic Press, Inc.

INTRODUCTION

Zeolitic aluminosilicates are extremely important materials as catalysts, adsorbents, and ion-exchanging substances. It is well established that the chemical and physical nature of zeolites depends on the crystal structure, Si/Al atomic ratio, and counter cation (1). Some chemical and, then, catalytic properties of zeolites are therefore considered to be understandable on the basis of the electronic structure of the elemental constituents: silicon, aluminum, oxygen, and cations. XPS (X-ray photoelectron spectroscopy) is considered to be one feasible technique for the understandings of the chemical nature of zeolites.

Several workers (2-11) have applied XPS techniques to zeolitic aluminosilicate systems. Except for transition-metal-exchanged zeolites (12), two important problems have been approached: surface composition and electronic state of each constituent element. With the surface compositions of Na-type zeolites, some groups indicated surface depletion of Al (5, 6), while other groups (3, 4) showed surface compositions equivalent to those of the bulk. FABMS (fast atom bombardment

mass spectra) (13) and AES (Auger electron spectroscopy) (14) techniques were also employed to study the surface composition of zeolites. These surface techniques indicated no dealumination in the surface layer of zeolites.

As for the electronic structure of zeolites, only a few detailed XPS studies (9-11) have been reported very recently. Barr *et al.* (11) have found that the BEs (binding energy) of the Si 2*p*, O 1*s*, Al 2*p*, and Na 2*s* or Ca 2*p* levels increase with decreasing Al/Si ratio or in an order of zeolite A < X < Y and with a cation exchange of Na⁺ to Ca²⁺ or to RE³⁺. On the basis of the patterns exhibited by the differences in BE of the core levels, they have suggested that the BE shifts are due to the complex subunits of the aluminosilicate system (Si-O and M⁺-Al-O) rather than simply due to the individual elements; aluminate subunits work as anionic groups, while silicate units as cationic groups. Similar dependencies of the core BEs of Al and Si have been reported by Wagner *et al.* (10) in their chemical state plots for A, X, and Y zeolites. On the other hand, Shyu and co-workers (9) have chosen the Si 2*p* band as a reference level for the purpose of charging correction

in their XPS study, resulting in relatively constant BE values for other constituents.

In the present report, we attempted to characterize the electronic structure of zeolites by a systematic XPS study of various zeolites as a function of the counter cation by using a series of alkali metal cations and as functions of zeolite composition and crystal structure by employing zeolites A, X, Y, and mordenites. The bonding nature

in zeolitic aluminosilicates is suggested on the basis of the XPS results. Some catalytic properties promoted by basic sites are demonstrated to be understood in terms of the basic strength of framework oxygen characterized by the O 1s BE.

EXPERIMENTAL

Materials. The zeolites featured in this study are described in Table 1 together with

TABLE 1
Surface Compositions of Zeolites

Zeolite	Si/Al atomic ratio in bulk	Degree of ion exchange (%)		Si 2s/Al 2p XPS intensity ratio	Si/Al ^a atomic ratio in surface
		Chemical analysis	XPS		
NaA (4A)	1.00			1.82	1.14
NaX (13X)	1.23			2.27	1.42
NaY (SK-40)	2.43			5.37	3.36
JRC-Z-Y4.8	2.38			4.29	2.68
Y5.6	2.78			4.54	2.84
M10 ^b	5.00			8.11	5.07
M15	7.69			12.0	7.50
M20	10.0			18.6	11.6
JRC-Z-HY4.8	2.63	99	>99	2.32	1.45
HY5.6	2.78	72	91	7.77	4.86
HM10 ^b	5.00	98	98	9.31	5.82
HM15	7.69	99	98	15.0	9.38
HM20	10.0	99	97	19.8	12.4
H-(Na)Y ^c	2.78		76	5.02	3.13
Li-(Na)Y	2.78		45	4.70	2.94
K-(Na)Y	2.78		51	4.42	2.76
Cs-(Na)Y	2.78		8.4	4.52 ^d	2.82
			34	5.17	3.23
			58	4.57	2.85
H-(Na)X ^c	1.23		78	2.80	1.75
Li-(Na)X	1.23		57	2.26	1.41
K-(Na)X	1.23		68	2.30	1.44
Cs-(Na)X	1.23		50	2.25 ^d	1.41

^a Relative atomic sensitivity is 1.60.

^b Mordenite.

^c JRC-Z-Y5.6 was employed.

^d The intensity of the Al 2p band was determined from the Al 2s intensity because of an overlapping of the Cs 4d and Al 2p bands (Al 2p/Al 2s = 0.70).

^e NaX (13X) was used.

their compositions. The JRC-Z series of zeolites were provided as fine powder reference catalysts by the Catalysis Society of Japan (15). HY and HM denote the corresponding decationized zeolites, which were prepared by catalyst suppliers by ion-exchanging Na^+ into NH_4^+ , followed by calcinations in air at 673 K for 2 h. The degrees of ion exchange are also summarized in Table 1. SK-40 (NaY; Nikka Seiko Co.), 13X (NaX; Gasukuro Kogyo Co., Lot. No. 980113), and 4A (NaA; Gasukuro Kogyo Co., Lot. No. 490338) were commercial zeolites. The composition (Si/Al) and ion-exchange degree of the zeolite were provided by manufacturers and part was confirmed by chemical analysis (Z-Y4.8 and 5.6). The composite oxides, SiO_2 (JRC-SIO-1) and Al_2O_3 (JRC-ALO-4), were also supplied by the Catalysis Society of Japan as reference catalysts (16).

Part of the Na^+ ions in JRC-Z-Y5.6 was ion-exchanged with alkali metal cations to produce Li-(Na)Y, K-(Na)Y, Cs-(Na)Y, and H-(Na)Y zeolites. The ion exchanges were carefully conducted at ca. 350 K using aqueous solutions of metal nitrates (Li^+ , K^+ , and Cs^+) or chloride (NH_4^+) to avoid surface dealumination; the pH of the solution was initially adjusted at 5.2–5.4 by varying the cation concentration. After the ion exchange, the zeolites were thoroughly washed and subsequently dried at 383 K for 24 h. NH_4 -(Na)Y was decomposed in air at 673 K for 2 h to prepare H-(Na)Y. A corresponding series of alkali metal cation-exchanged X zeolites was similarly prepared. The high crystallinity of the zeolite examined here was confirmed by an X-ray powder diffraction technique (Shimazu VD-1).

Procedures. XP spectra of the zeolites were measured on a Hitachi 507 photoelectron spectrometer equipped with a cylindrical mirror analyzer by utilizing an Al anode (1486.6 eV, 9 kV, 50 mA). The spectrometer was calibrated using the Fermi level (0.0 eV) and Pd $3d_{5/2}$ band (335.5 eV) for Pd metal. The instrumental resolution expressed by the FWHM (full width at half-

maximum) of Au $4f_{7/2}$ was 2.1 eV for gold metal.

The zeolite sample was mounted on a copper sample holder by utilizing a double-cohesive tape, followed by an evacuation at room temperature in a pretreatment chamber to ca. 1×10^{-3} Pa. The sample was subsequently transferred to an XPS analyzer chamber for the measurements of the XP spectra. The base pressure in the analyzer was usually maintained at ca. 1×10^{-5} Pa during the measurements.

All the BEs were referenced to the C 1s level at 285.0 eV due to adventitious carbon. The reproducibility of the BEs thus determined was usually ± 0.15 eV. The peak area intensities were evaluated by planimetry of the graphic displays of the spectra by assuming linear base lines.

RESULTS AND DISCUSSION

The XPS results on the zeolites are summarized in Tables 1 and 2 for the surface compositions and BEs of the constituent elements, respectively. The FWHM values of the Si $2s$, Si $2p$, Al $2p$, and O $1s$ levels for the zeolites and SiO_2 were usually 3.2, 2.6, 2.4, and 2.8 ± 0.15 eV, respectively, being nearly independent of the crystal structure, bulk composition, and cation(s) with the present spectrometer. The alumina, however, provided broadened FWHMs by ca. 0.5 eV for the Al $2p$ and O $1s$ levels.

Surface Composition

One performs XPS studies to reveal the electronic structure of zeolites and furthermore to compare it with their chemical properties. For these purposes one is required to examine that the surface properties of zeolites are nearly identical with those of the bulk: no significant surface destruction, surface dealumination, or surface accumulation of impurities.

In the present study the Si $2s$ and Al $2p$ levels were used for the evaluation of the surface composition of the zeolite, taking into consideration critical superpositions of the bremsstrahlung Al KLL Auger peak

TABLE 2
XPS Binding Energies for Zeolites

Zeolite	Al/Si atomic ratio	Binding energies (eV) ^a					
		Si 2s	Si 2p	Al 2p	Na 1s	O 1s	Other bands
NaA (4A)	1.00	152.8	101.7	73.7	1072.0	531.0	
NaX (13X)	0.81	153.0	101.9	74.1	1071.9	531.1	
NaY (SK-40)	0.41	153.6	102.5	74.2	1072.1	531.8	
JRC-Z-Y4.8	0.42	153.6	102.6	74.2	1072.2	531.8	
Y5.6	0.36	153.6	102.5	74.2	1072.4	532.0	
M10 ^b	0.20	153.6	102.5	74.1	1072.4	532.0	
M15	0.13	154.0	103.0	74.1	1072.6	532.3	
20	0.10	154.0	103.1	74.1	1072.3	532.3	
JRC-Z-HY4.8	0.38	153.9	102.8	74.9		532.3	
HY5.6	0.36	154.1	103.0	74.6	1072.7	532.6	
HM10 ^b	0.20	153.8	102.7	74.0		532.2	
HM15	0.13	154.0	102.9	74.1		532.5	
HM20	0.10	154.2	103.2	74.2		532.8	
JRC-SIO-1	0.0	154.0	103.1			532.5	
ALO-4				74.0		530.9	Al KLL = 1387.8 ^g
H-(Na)Y ^c	0.36	154.0	103.1	74.6	1072.3	532.5	
Li-(Na)Y	0.36	153.8	102.7	74.5	1072.3	532.2	Li 1s = 55.9
K-(Na)Y	0.36	153.6	102.5	74.0	1072.1	531.9	K 2p _{3/2} = 293.6
Cs-(Na)Y (8.4) ^d	0.36	153.6	102.5	74.0 ^e	1072.2	531.9	Cs 3d _{5/2} = 725.2
(34)		153.7	102.6	74.0	1071.9	531.8	725.2
(58)		153.3	102.3	74.0	1072.1	531.5	724.9
H-(Na)X ^f	0.81	153.8	102.7	74.9	1072.4	532.2	
LI-(Na)X	0.81	153.5	102.4	74.1	1072.1	531.6	Li 1s = 55.7
K-(Na)X	0.81	153.0	102.0	74.0	1071.8	531.3	K 2p _{3/2} = 293.5
Cs-(Na)X	0.81	152.8	101.7	73.8 ^e	1071.5	530.9	Cs 3d _{5/2} = 724.8

^a Referenced to C 1s = 285.0 eV.

^b Mordenite.

^c JRC-Z-Y5.6 was employed.

^d Degree of ion exchange.

^e The Al 2p BE was estimated from the Al 2s BE because of an overlapping of the Al 2p and Cs 4d bands (Al 2s - Al 2p = 44.9 eV).

^f NaX (13X) was employed.

^g Kinetic energy (eV).

(17) and the Si 2p band and of the Si 2s energy-loss spectrum and the Al 2s band. The following equation was employed to evaluate the surface composition from the Si 2s/Al 2p intensity ratio,

$$R = \left(\frac{I_j}{I_i} \right) = \frac{S_j \lambda_j \sigma_j}{S_i \lambda_i \sigma_i} \cdot \frac{n_j}{n_i} = \left(\frac{I_j}{I_i} \right)_0 \frac{n_j}{n_i},$$

$i = \text{Al } 2p \text{ and } j = \text{Si } 2s, \quad (1)$

where S is an analyzer transmission function. λ , σ , and n denote the escape depth of photoelectrons, the atomic cross section for ionization, and the concentration of an element of interest, respectively. The λ values calculated by Penn (18) and atomic cross sections by Scofield (19) were employed here. The relative atomic sensitivity, $(I_{\text{Si } 2s}/I_{\text{Al } 2p})_0$ in Eq. (1), thus obtained

was 1.60. Comparing theoretical (19, 20) and experimental (21, 22) relative atomic sensitivities, the Si/Al atomic ratios are estimated to be precise within an accuracy of ca. 10%.

Taking into consideration the accuracies of the theoretical sensitivity and XPS intensity ratio, it is concluded from Table 1 that with the Na-type zeolites the surface Al concentration is very close to that of the bulk, but perhaps slightly depleted. SK-40, however, seems to be significantly dealuminated in the surface. The difference between the zeolites is deemed to be due primarily to the differences in sample preparation and pretreatment methods, although scatterings in the intensity data among the workers (23) may not be ignored. With ZSM-5 (7, 8) and ZSM-11 (8) zeolites, it has been recently reported that surface compositions depend on the particle size and crystal morphology.

As for the surface compositions of JRC-H-type zeolites except HY 4.8, it is evident that significant surface dealumination occurs in industrial decationizing procedures. The superficial Al impoverishments are also observed by other workers (3, 13). ^{29}Si MASNMR (24) studies on the JRC series of zeolites have indicated only a slight dealumination of Y5.6 zeolite with the ion exchange; the Si/Al ratio by MASNMR is 3.0 for HY5.6, which is comparable to 2.7 for Y5.6. No dealumination of the morденite was detected by MASNMR (24, 25). The differences between the XPS and the MASNMR observations suggested that the surface layers are more extensively dealuminated than the bulk of the zeolite. Selective surface dealuminations are also reported for EDTA treatments of zeolites (9).

The zeolite HY4.8 showed reversed XPS results; apparent surface enrichment of aluminum is shown in Table 1. However, an extensive increase in the Si/Al atomic ratio by MASNMR (from 2.8 to 5.9 (25) or from 2.7 to 4.8 (24) on the ion exchange) indicates a significant dealumination from the

zeolite framework. Furthermore, ^{29}Al MASNMR (25) for HY4.8 clearly showed the presence of large amounts of octahedrally coordinated aluminum and free aluminum species in tetrahedral surroundings in addition to the framework aluminum. Accordingly, it is concluded that in HY4.8 zeolite, detached aluminum species are enriched in the surface region of the zeolite. Defosse *et al.* (6) showed a superficial segregation of Al in a HY zeolite calcined at 1173 K. The difference among the zeolites may be ascribable to preparation effects. It is demonstrated that XPS and MASNMR techniques are complementary in the investigation of zeolites.

With the alkali metal cation-exchanged Y5.6 zeolites, no significant surface dealumination was observed as shown in Table 1. This is due to relatively high pH values of the ion-exchanging solution. Their degrees of ion exchange in surface layers are summarized in Table 1.

Electronic Structure

(1) *Effect of zeolite composition.* The Na-type zeolites were examined first to show the effect of the zeolite composition on the electronic structure. The BE of the O 1s level is shown in Fig. 1 as a function of the Al/Si atomic ratio in the bulk; the O 1s BE decreases with increasing Al content. It is also evident from Table 2 that the BEs of the Si 2p, Na 1s, and Al 2p bands decrease with an increase in the Al/Si ratio. Accord-

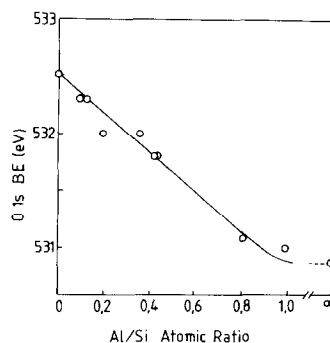


FIG. 1. Correlation between the binding energy of the O 1s band and the Al/Si atomic ratio.

ingly, with the Na-type zeolites, the BE values are delineated by the zeolite composition regardless of the crystal structure. The chemical shift between Al/Si = 0 and 1 depends strongly on the constituting element and decreases in the order O 1s (1.6 eV) > Si 2s (1.2 eV) > Na 1s (0.5 eV) > Al 2p (0.3 eV).

The present results in Table 2 are consistent with fragmentary observations of other workers. With zeolites NaA, NaX, and NaY, Barr *et al.* (11) and Wagner *et al.* (10) have reported the chemical shifts for the elemental constituents between A and Y zeolites: 1.4 (10, 11), 0.7–0.9 (10, 11), 1.25 (11), and 0.95 eV (11) for Si 2p, Al 2p, O 1s, and Na 2s levels, respectively. Vinek *et al.* (2) have also shown that $\Delta BE = 0$ for the Al 2p band between NaX and NaY, while $\Delta BE = 1.8$ and 0.6 eV for the Si 2p and O 1s bands, respectively. Although the sizes of chemical shifts are thus rather scattered among the workers, it is demonstrated that all the BEs decrease as the Al content increases and that the chemical shifts for the silicon and oxygen are larger than those for sodium and aluminum. Similar observations have been made by the X-ray emission studies by Patton *et al.* (26) for a variety of zeolites including A, X, Y, rho, offretite, erionite, and mordenite; the chemical shift ΔSiK_{β} is two times larger than the ΔAlK_{β} and the chemical shifts are simply correlated to the Al content in the materials.

The XPS chemical shift (ΔBE) of a core level is approximately described as (27)

$$\Delta BE = k\Delta q - \Delta V, \quad (2)$$

where Δq denotes a change in the charge density. k is a proportional constant and represented by e^2/r (r , radius of valence shell) in a simplified model. ΔV shows the changes in Madelung potential and relaxation energies. As for zeolite systems, ΔV may be expected to change with the Al content and counter cation due to the electric field generated by cations and negative charges on zeolite frameworks. However,

it seems difficult to estimate the magnitude of electric field effects on the BE values. One of the common ingredients constituting the zeolites, whose electronic state is considered to be relatively invariant, may be chosen as a reference element to reduce the effects of ΔV on ΔBE instead of the C 1s band. However, all the BE values for the constituent elements shift linearly with the composition. Therefore, the same conclusions can be reached for relative chemical properties of the zeolites despite reduced sizes of the chemical shifts (e.g., by ca. 0.5 eV at maximum between the zeolites with Al/Si = 1 and 0 when referenced to the Na 1s band). The chemical shifts calculated by using the C 1s level are, accordingly, employed herein for further discussions. The adequacy of the C 1s band as a reference level in zeolite systems has been shown by Barr *et al.* (11).

From the results in Table 2, it is concluded that the positive charge on silicon is reduced with increasing aluminum content, while the negative charge on oxygen is enhanced. The charge density on aluminum seems to vary slightly with the zeolite composition. It is likely that the apparent small chemical shift of the Al 2p band is due to Madelung energy shift. A rather invariant charge density on aluminum atoms seems very natural, taking into consideration Loewenstein's rule (1) in zeolite systems which predicts that $(AlO_2)^-$ is always surrounded by four (SiO_2) units. The ^{29}Al MASNMR data (24) for the present Na-type zeolites confirmed the existence of a single type of aluminum.

(2) *Effect of cation.* Both Y and X zeolites were ion-exchanged with a series of alkali metal cations to examine systematically the effect of cation on the electronic structure of the zeolites. JRC-Z-Y5.6 was chosen as a starting NaY zeolite, since the bulk and surface compositions are almost identical as shown in Table 1. As mentioned above, the surface composition was not altered by replacing Na^+ with the other cation. In order to avoid surface destruc-

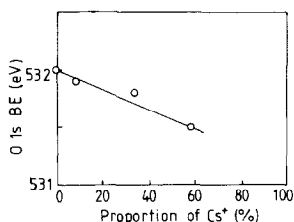


FIG. 2. Dependency of the O 1s binding energy for Cs-(Na)Y zeolite on the proportion of Cs⁺ in the zeolite.

tion by repeated ion-exchanging procedures, the degree of cation exchange was kept rather low and at ca. 50–60%.

The effect of the extent of ion exchange on the O 1s BE is depicted in Fig. 2 for Cs-(Na)Y zeolites. The variation in FWHM of the XPS signal was not observed within an accuracy of ± 0.15 eV. Apparently, the BE decreases with increasing proportion of Cs⁺ cation. Similar observations were made for the Al and Si bands.

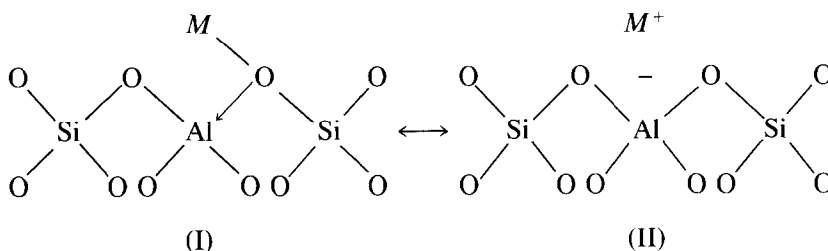
Figure 3 shows the O 1s BE for the alkali metal cation-exchanged X and Y zeolites as a function of the electronegativity (χ_i) of the cation. The results for decationized zeolites are also included. It is revealed that the BE increases with increasing χ_i of the counter cation in zeolite and that the BE differences between the Y and X zeolites are kept nearly constant when compared at a similar degree of ion exchange. With the Si 2s, Na 1s, and Al 2p BEs, analogous observations

were made as listed in Table 2. However, the chemical shifts of the Al 2p and Na 1s bands are smaller than those of the O 1s and Si 2s levels and are close to each other. These results extend the observations made by Barr *et al.* (11). Consequently, it is concluded that the electronic structure of zeolite strongly depends on both the Al content and the cation involved, regardless of the crystalline structure.

With the O 1s band, the BE diminishes with increasing Al content and with decreasing χ_i of the cation in the zeolite. As suggested from Eq. (2) the decrease in the O 1s BE indicates the augmentation in the electron density of oxygen atoms and vice versa. A good correlation between the BE of the N 1s band and basicity is well established for a wide variety of organic compounds containing nitrogen (28). Therefore, it is demonstrated that the basic strength of lattice oxygen in zeolite enhances as the Al content increases and as χ_i of cation decreases.

All the BEs for JRC-H series zeolites are greatly increased by decationizing as shown in Table 2. These shifts are explained in terms of extensive surface dealuminations as discussed above and in terms of the increased χ_i of cation by ion-exchanging Na⁺ to H⁺.

(3) *Nature of Bonding in Zeolites.* In order to describe properly the electronic feature of zeolites, a bonding model is proposed:



In state (I) covalent bonds between a cation and an oxygen are formed and stabilized by a coordination of oxygen lone pair

electrons to an adjacent coordinatively unsaturated Al³⁺ (Lewis acid). The symmetrical and identical counterpart is also con-

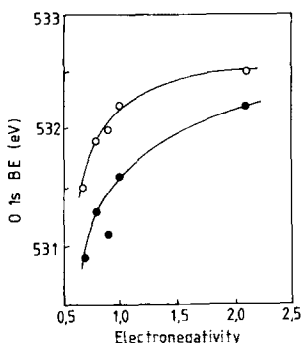


FIG. 3. Dependencies of the O 1s binding energy for the X and Y zeolites on the electronegativity of cation (●) X and (○) Y.

structured by utilizing another Si–O–Al bond in state (I). Another bonding structure is represented by an ionic state (state (II)), which is usually used to explain some characteristics of zeolites. The negative charge on aluminum is assumed to be fairly delocalized over the framework. The actual bonding nature is described as a resonance hybrid between these two extremes.

The electronic structure of zeolites revealed by the present XPS results is interpretable on the basis of the above model. With the decreasing χ_i of cation, $H^+ > Li^+ > Na^+ > K^+ > Cs^+$, the covalency of the bond between oxygen and cation is expected to decrease (29) and, accordingly, ionic state (II) becomes prevailing, resulting in the enhanced electron densities on electronegative constituents in the framework; oxygen and silicon atoms (29, 30). When the content of Al increases in zeolite with a fixed cation species, the concentration of the cation correspondingly increases, causing augmented electron densities on the zeolitic framework. Consequently, the covalent bonding between cation and lattice oxygen is pointed out herein to be important to understand the electronic structure of zeolite as well as the ionic bondings. The bonding model proposed above explains also the group-shift behavior (11) in the XPS BEs.

The CNDO/2 calculations of Beran and co-workers (31) for the zeolite clusters may substantiate the proposed bonding nature of zeolite: (i) the bond order of Al–O is considerably lower than that of Si–O, this being consistent with the assumption of the existence of rather weak $O \rightarrow Al$ coordination bonds in the covalent model and (ii) the charge density on sodium is fairly low (ca. 0.25 e), this suggesting the covalent nature of Na^+ zeolite bondings.

(4) *Catalytic properties of alkali metal cation zeolites.* The electronic structure of zeolites featured above by XPS is anticipated to explain some of the chemical nature of zeolites, for example, certain catalytic properties. Vinek *et al.* (2) suggested a correlation between the BE of Mg 2s band and catalytic activities of Mg^{2+} -exchanged X and Y zeolites for certain reactions over acidic sites. In the present study, catalytic properties promoted by basic sites are compared with the electronic structure of zeolites. The basic sites are conjectured to be lattice oxide anions when completely dehydrated.

According to Yashima *et al.* (32), a NaX zeolite shows higher catalytic activities than a NaY zeolite for dehydrogenation of isopropyl alcohol, a characteristic reaction promoted by basic sites. This reaction is extensively enhanced by exchanging Na^+ ions into K^+ , Rb^+ , or Cs^+ , whereas the reaction is depressed by an introduction of Li^+ . The alkylation of methyl group of toluene by methanol or formaldehyde, which is a representative reaction over basic sites, is effectively catalyzed by the alkali metal cation X and Y zeolites (33, 34). The activity to ethylbenzene is in the order $Li^+ < Na^+ < K^+ < Cs^+$ for the both types of zeolite and the X-type zeolites show higher activities than the corresponding Y-type zeolites. These results are just the behaviors anticipated from the aforementioned basic strength of lattice oxygen in the ion-exchanged zeolites. The temperature of decomposition of $Mo(CO)_6$ engaged in the zeolite, which is characteristic of basic oxides

such as Al_2O_3 and MgO (35), has also been found to be well delineated by the O 1s BE value in Table 2; the decomposition temperature is reduced with the decreasing O 1s BE of the zeolite (36).

Consequently, some of the catalytic properties of the alkali metal cation-exchanged zeolites seem to be well understood in terms of the electronic structure characterized by XPS.

REFERENCES

- (a) Thomas, J. M. "Chemistry and Physics of Solid Surfaces VI" (R. Vanselow and R. Howe, Eds.), p. 107. Springer-Verlag, Berlin, 1986; (b) Gates, B. C., Katzer, J. R., and Schuit, G. C. A., "Chemistry of Catalytic Processes," p. 49. McGraw-Hill, New York, 1979; (c) Maxwell, I. E., "Advances in Catalysis" (D. D. Eley, P. W. Selwood, and P. B. Weisz, Eds.), Vol. 31, p. 1. Academic Press, San Diego, 1982.
- Vinek, H., Noller, H., and Ebel, M., *Z. Phys. Chem. N. F.* **103**, 325 (1976).
- Finster, J., and Lorenz, P., *Chem. Phys. Lett.* **50**, 223 (1977).
- Adams, J. M., Evans, S., Reid, P. I., Thomas, J. M., and Walters, M. J., *Anal. Chem.* **49**, 2001 (1977).
- (a) Tempere, J.-Fr., Delafosse, D., and Contour, J. P., *Chem. Phys. Lett.* **33**, 95 (1975); (b) "Molecular Sieves II" (J. R. Katzer, Ed.), ACS Symp. Ser. Vol. 40, p. 76. 1977.
- Defosse, C., Delmon, B., and Canesson, P., "Molecular Sieve II" (J. R. Katzer, Ed.), ACS Symp. Ser. Vol. 40, p. 86. 1977.
- Derouane, E. G., Gilson, J. P., Gabelica, Z., Mousty-Desbuquoit, C., and Verbist, J., *J. Catal.* **71**, 447 (1981).
- Auroux, A., Dexpert, H., Leclercq, C., and Vedrine, J., *Appl. Catal.* **6**, 95 (1983).
- Shyu, J. Z., Skopinski, E. T., Goodwin, J. G., and Sayari, A., *Appl. Surf. Sci.* **21**, 297 (1985).
- Wagner, C. D., Six, H. A., Jansen, W. J., and Taylor, J. A., *Appl. Surf. Sci.* **9**, 203 (1981).
- (a) Barr, T. L., *Appl. Surf. Sci.* **15**, 1 (1983); (b) Barr, T. L., and Lishka, M., *J. Amer. Chem. Soc.* **108**, 3178 (1986).
- e.g., (a) Vedrine, J. C., Dufaux, M., Naccache, C., and Imelik, B., *J. Chem. Soc. Faraday Trans. 1* **74**, 440 (1978); (b) Gallezot, P., *Catal. Rev. Sci. Eng.* **20**, 121 (1979), and references therein; (c) Okamoto, Y., Ishida, N., Imanaka, T., and Teranishi, S., *J. Catal.* **58**, 82 (1979); (d) Pedersen, L. A., and Lunsford, J. H., *J. Catal.* **61**, 39 (1980).
- Dwyer, J., Fitch, F. R., Qin, G., and Vickerman, J. C., *J. Phys. Chem.* **86**, 4574 (1982).
- Suib, S. L., Stucky, C. D., and Blattner, R. J., *J. Catal.* **65**, 174 (1980).
- Hattori, T., Matsumoto, H., and Murakami, Y., "Fourth Intern. Symp. Preparation of Heterogeneous Catalysts, Louvain-la-neuve, 1986."
- (a) Murakami, Y., "Preparation of Catalysts, III" (G. Poncelet, P. Grange, and P. A. Jacobs, Eds.), p. 775. Elsevier, Amsterdam, 1983; (b) Okamoto, Y., Oh-Hara, M., Maezawa, A., Imanaka, T., and Teranishi, S., *J. Phys. Chem.* **90**, 2396 (1986).
- Castle, J. E., Hazell, L. B., and Whitehead, R. J., *J. Electron Spectrosc. Relat. Phenom.* **9**, 247 (1976).
- Penn, D. R., *J. Electron Spectrosc. Relat. Phenom.* **9**, 29 (1976).
- Scofield, J. H., *J. Electron Spectrosc. Relat. Phenom.* **8**, 129 (1976).
- Nefedov, V. I., Sergushin, N. P., Band, I. M., and Trzhaskovskaya, M. B., *J. Electron Spectrosc. Relat. Phenom.* **2**, 383 (1973).
- Wagner, C. D., Davis, L. E., Zeller, M. V., Taylor, J. A., Raymond, R. H., and Gale, L. H., *Surf. Interface Anal.* **3**, 211 (1981).
- Evans, S., Pritchard, R. G., and Thomas, J. M., *J. Electron Spectrosc. Relat. Phenom.* **14**, 341 (1978).
- Madey, T., Wagner, C. D., and Joshi, A., *J. Electron Spectrosc. Relat. Phenom.* **10**, 359 (1977).
- Nakata, S., Soma, M., and Asaoka, S., "7th Meeting of Reference Catalysts, Catalysis Society of Japan, Hamamatsu, 1984," No. 13.
- Suzuki, K., Hayashi, S., Kiyozumi, Y., Arata, S., Hayami, K., and Yamamoto, O., "7th Meeting of Reference Catalysts, Catalysis Society of Japan, Hamamatsu, 1984," No. 12.
- Patton, R. L., Flanigen, E. M., Dowell, L. G., and Passoja, D. E., "Molecular Sieves II" (J. R. Katzer Ed.), ACS Symp. Ser. Vol. 40, p. 64. 1977.
- Carlson, T. A., "Photoelectron and Auger Spectroscopy." Plenum, New York, 1975.
- Mills, B. E., Martin, R. L., and Shirley, D. A., *J. Amer. Chem. Soc.* **98**, 2380 (1976).
- Pauling, L., "The Nature of the Chemical Bond." Cornell Univ. Press, New York, 1960.
- Tanaka, K., Ozaki, A., and Tamaru, K., *Shokubai (Catalysts)* **6**, 262 (1964).
- (a) Beran, S., and Dubsky, J., *J. Phys. Chem.* **83**, 2538 (1979); (b) Beran, S., Jiru, P., and Wichterlova, B., *J. Phys. Chem.* **85**, 1951 (1981).
- Yashima, T., Suzuki, H., and Hara, N., *J. Catal.* **33**, 486 (1974).
- Yashima, T., Sato, K., Hayasaka, T., and Hara, N., *J. Catal.* **26**, 303 (1972).
- Itoh, H., Miyamoto, A., and Murakami, Y., *J. Catal.* **64**, 284 (1980).

35. e.g., (a) Brenner, A., and Burwell, R.L., *J. Amer. Chem. Soc.* **97**, 2565 (1975); (b) Brenner, A., and Burwell, R. L., *J. Catal.* **52**, 353 (1978); (c) Howe, R. F., Davidson, D. E., and Whan, D. A., *J. Chem. Soc. Faraday Trans. 1* **68**, 2266 (1972).
36. (a) Maezawa, A., Kane, H., Okamoto, Y., and Imanaka, T., *Chem. Lett.*, 241 (1988); (b) Okamoto, Y., Maezawa, A., Kane, H., Mitsushima, I., and Imanaka, T., *J. Chem. Soc. Faraday Trans. 1* **84**, 851 (1988); (c) Okamoto, Y., Maezawa, A., Kane, H., and Imanaka, T., "Proceedings, 9th International Congress on Catalysis" (Phillips, M. J. and Ternan, M., Eds.), Vol. 1, 11 (1988).